Published in final edited form as:
Environ Sci Technol. 2013 October 1; 47(19): 11232–11240. doi:10.1021/es403377p.

The Stability of Silver Nanoparticles in a Model of Pulmonary Surfactant

Leo Bey Fen[1,2], **Shu Chen**[1], **Yoshihiko Kyo**[1], **Karla-Luise Herpoldt**[1], **Nicholas J. Terrill**[3], **Iain E. Dunlop**[1], **David S. McPhail**[1], **Milo S. Shaffer**[4], **Stephan Schwander**[5], **Andrew Gow**[6], **Junfeng (Jim) Zhang**[7], **Kian Fan Chung**[8], **Teresa D. Tetley**[8], **Alexandra E. Porter**[1,*], and **Mary P. Ryan**[1,*]

[1]Department of Materials and London Centre for Nanotechnology, Imperial College London, Exhibition Road, London SW7 2AZ, UK

[2]Department of Mechanical Engineering, Faculty of Engineering Building, University of Malaya, Kuala Lumpur 50603, MALAYSIA

[3]Diamond Light Source Ltd., Diamond House, Harwell Science and Innovation Campus, Didcot, Oxfordshire OX11 0DE, United Kingdom

[4]Department of Chemistry and London Centre for Nanotechnology, Imperial College London, Exhibition Road, London SW7 2AZ, UK

[5]Department of Environmental and Occupational Health, University of Medicine and Dentistry (UMDNJ) School of Public Health, New Jersey, USA

[6]Department of Pharmacology and Toxicology at Rutgers University, Piscataway, NJ, USA

[7]Department of Preventive Medicine, Keck School of Medicine, University of Southern California, USA

[8]National Heart and Lung Institute, Imperial College London, UK

Abstract

The growing use of silver nanoparticles (AgNPs) in consumer products has raised concerns about their potential impact on the environment and human health. Whether AgNPs dissolve and release Ag^+ ions, or coarsen to form large aggregates, is critical in determining their potential toxicity. In this work, the stability of AgNPs in dipalmitoylphosphatidylcholine (DPPC), the major component of pulmonary surfactant, was investigated as a function of pH. Spherical, citrate-capped AgNPs with average diameters of 14 ± 1.6 nm (n=200) were prepared by a chemical bath reduction. The kinetics of Ag^+ ion release was strongly pH-dependent. After 14 days of incubation in sodium perchlorate ($NaClO_4$) or perchloric acid ($HClO_4$) solutions, the total fraction of AgNPs dissolved varied from ~10 % at pH 3, to ~2 % at pH 5, with negligible dissolution at pH 7. A decrease in pH from 7 to 3 also promoted particle aggregation and coarsening. DPPC (100 $mg.L^{-1}$) delayed the

*Corresponding Authors: m.p.ryan@imperial.ac.uk; phone: (+44)2075946755; fax: (+44)2075945017. a.e.porter@imperial.ac.uk; phone: (+44)2075949691; fax: (+44)2075945017.

Supporting Information. Experimental protocols, schematic of procedure to measure particle size, ICP, zeta-potential and SAXS of AgNPs after various incubation conditions. This material is available free of charge via the internet: http://pubs.acs.org.

release of Ag^+ ions, but did not significantly alter the total amount of Ag^+ released after two weeks. In addition, DPPC improved the dispersion of the AgNPs and inhibited aggregation and coarsening. TEM images revealed that the AgNPs were coated with a DPPC layer serving as a semi-permeable layer. Hence, lung lining fluid, particularly DPPC, can modify the aggregation state and kinetics of Ag^+ ion release of inhaled AgNPs in the lung. These observations have important implications for predicting the potential reactivity of AgNPs in the lung and the environment.

Keywords

silver nanoparticles (AgNPs); dipalmitoylphosphatidylcholine (DPPC); aggregation; dissolution; toxicity

INTRODUCTION

Engineered silver nanoparticles (AgNPs) have attracted the attention of scientists for their remarkable properties, including their excellent electrical and thermal conductivity, as well as unique optical and antimicrobial properties.[1–5] However, due to the large production volume of manufactured AgNPs, in particular airborne products (e.g. disinfectant sprays) and a variety of consumer products (e.g. washing machine, water purification and air filters, toothpaste and deodorants), Ag may be released into the environment either as soluble ions, nanoparticles (NPs) or NP aggregates, during handling, washing, disposal or abrasion.[6] Since AgNPs are prevalent in consumer products, these release routes raise concerns about potential toxic effects of AgNPs on the environment and human health.[7]

Inhalation of airborne NPs is one of the main exposure routes by which NPs can enter the human body. After inhalation, relatively large particles or agglomerates (diameter > 1 μm) are likely trapped in the mucus of the upper airways and removed by the mucociliary escalator. However, NPs with a diameter < 20 nm are likely to escape the mucus trapping and enter the deepest zone of lung: the alveolar region.[8,9, 10] The deep lung is comprised of a monolayer of type I and type II epithelial cells which allow gas exchange and also directed transmigration of cells such as macrophages that form part of the lung's immune system. The deep lung also consists of a layer of lung-lining fluid (LLF), pulmonary surfactant composed of 90% phospholipids and 10 % surfactant proteins[11]. The most abundant phospholipids are based on phosphatidylcholine (PC), 41–70% of which is DPPC.

The LLF plays an important role in regulating the immunity of the lung.[12, 13] The DPPC-enriched monolayer functions to produce near-zero surface tension at the end of exhalation, easing the work of breathing and preventing the alveoli from collapsing.[14, 15] There are four lamellar phases recognised in saturated phosphatidylcholines (e.g. DPPC), see SI. At 37 °C, DPPC monolayers are rigid enough to be compressed to high surface pressure (π>50 $mN.m^{-1}$) or low surface tension (γ=0 $mN.m^{-1}$) and can sustain this low surface tension for a considerable time without collapsing.[16, 17] Lung surfactant deficiency and dysfunction may lead to the severe pulmonary disorders such as (acute) respiratory distress syndrome (RDS).[18]

The molecular structure of DPPC contains a hydrophilic and a hydrophobic end (Figure 4). The zwitterionic trimethyl ammonium and acidic phosphate head of the molecule is hydrophilic, while the two long chain fatty acid tails esterified to the glycerol are lipophilic and hydrophobic. Hydrogen bonding and electrostatic interactions control the interaction between DPPC and AgNPs/citrate. It is well established that lipid vesicles do not rupture to form a bilayer on metal surfaces.[19] To confirm the formation of a lipid bilayer on AgNPs/citrate, McConnell's group[20] created supported lipid bilayers by spreading lipid vesicles on hydrophilic supports. DPPC-NPs interactions depend on several factors, such as particle size,[21] surface charge[22] and particle nature (hydrophilic or hydrophobic).[23]

Several studies have compared the colloidal stability of NPs in different media, including rat bronchoalveolar lavage (BAL);[24] phosphate buffered saline (BAL mimic containing bovine serum albumin (BSA) and DPPC);[25, 26] semisynthetic lung fluid (DPPC/palmitoyl-oleoyl-phosphatidylglycerol/surfactant protein B (SP-B); 70:30:1 wt %).[27] These studies found that NPs were well-dispersed in the presence of DPPC and proteins, and that synthetic lung fluid was as effective as BAL in dispersing NPs. Here, we have studied the interaction of AgNPs with DPPC and isolated the effects of DPPC – the major component of LLF. We specifically chose not to include other proteins presented in the LLF as some of these components (e.g. SP-A, SP-B and SP-D) contain sulphur. This may lead to desulphurisation of proteins by AgNPs and formation of Ag_2S. The sulphurisation process would confound the analysis of ICP and TEM and make it difficult to draw accurate conclusions about the mechanisms by which pH affect the stability of the NPs.

Interactions occurring between biological media and NPs are expected to govern the subsequent biological effects of the particles. For respirable NPs, interactions with LLF components as well as local cell populations will determine the effects on cell metabolism and lung function.[28] Hence, it is important to understand how NPs behave in different biological media, to predict downstream effects. The effects of the LLF on the aggregation state of NPs will play an important role in determining the interaction of particles with proteins, cells and tissues. An altered aggregation state will modify particle transport, the amount of AgNPs internalised by cells, subsequent interactions within cells[29], and can also alter the surface tension of the LLF and affect immune responses by sequestering lipids or proteins.[30] These factors may impact the bioavailability of AgNPs, cellular toxicity and even lung function.[31]

The detailed mechanisms by which AgNPs damage cells and tissues are not fully understood; however, recent studies indicate that Ag^+ ion release is a major pathway underlying AgNPs bio-reactivity and toxicity.[32,33] Ionic silver (Ag^+), a well-known oxidation catalyst, is implicated in protein damage by desulphurisation, generates reactive oxygen species (ROS)[34] and may interfere with NO redox equilibria in the lung.[35] This oxidative potential may increase the permeability of the lung epithelium to AgNPs resulting in DNA damage, lipid membrane damage, chromosomal aberrations, and cell-cycle arrest.[7, 8] Through these biochemical pathways, release of Ag^+ ions is a critical process that will determine the downstream effects of AgNPs on human health.[36, 37, 38]

The aim of this study was to investigate the impact of DPPC on the stability of AgNPs with well-controlled physicochemical properties. The influence of phospholipids on the aggregation state and release of Ag^+ ions at various pH conditions, representative of environments found in the lung, have been investigated. Consideration of any feedback processes (*i.e.* how components of the LLF affect the physicochemical properties and reactivity of NPs) in such systems is an important aspect of understanding the impact of nanomaterials on cell toxicity.

MATERIALS AND METHODS

Ag NPs were prepared by chemical bath deposition from $AgNO_3$ solution as described in supplementary information.

Effect of pH and DPPC on stability of AgNPs

DPPC was purchased from Sigma Aldrich, UK (catalogue number P0763). The effect of pH on the stability of AgNPs (25 mg L^{-1}) was studied for 0 and 100 mg L^{-1} DPPC, in perchlorate acid solutions (pH 3, 5 and 7) by bath sonication for 10 minutes. Samples were incubated at 37°C with reaction times between 1 and 336 hours (2 weeks) in a dri-block heater.

To minimise the impact of anions on the stability of the AgNPs, non-interacting buffers were used and perchloric acid (Sigma-Aldrich), was used to adjust the pH. The pH was adjusted using either 0.1 M sodium perchlorate ($NaClO_4$) or perchloric acid ($HClO_4$) solutions. pH 5 and 7 were chosen to correspond approximately to lysosomal and extracellular media pH, respectively; pH 3 was chosen as a positive control.

Analytical methods

The samples were analysed using a range of complimentary techniques summarised below; full details of the experimental protocols are provided in the supplementary information:

Transmission electron microscopy (TEM) was performed using a JEOL 2010 TEM to determine particle size distribution, aggregation state and crystallinity (selected area electron diffraction);

Inductively Coupled Plasma–Optical Emission Spectroscopy (ICP-OES) was used to determine the amount of dissolved Ag into the test media at various time points.

Energy dispersive X-ray (EDS) The presence of DPPC and cleanliness of synthesised particles was examined using EDS in the JEOL 2010.

Zeta potential (ξ) *measurements* were performed using a ZetaPALS (Brookhaven Instruments Corporation, USA) to determine the surface charge on the particles as-prepared and post exposure to DPPC as a function of pH.

Small Angle X-ray Scattering (SAXS) was performed on the I22 beamline at the Diamond Light Source, UK to provide an *in-situ* correlative measure of particle size and aggregation state.

RESULTS

AgNP Preparation and Characterisation

A bright-field TEM image of as-prepared AgNPs is shown in Figure 1a. The particles were spherical in morphology with an average diameter of 14 ± 1.6 nm (n=200) as characterized by TEM. SAED patterns (Figure 1c) revealed that as-synthesised NPs have characteristic lattice spacings 0.236 nm, 0.204 nm, and 0.145 nm, corresponding to the (111), (200) and (220) planes of metallic silver (Ref.#01-087-0597). EDS analysis confirmed that sulfidation of AgNPs had not occurred and all impurities had been removed after 3x washing with DI water. The ξ value of the as-synthesised AgNPs/citrate was −17.9 ± 3.0 mV. This negative surface charge is consistent with the electrostatic stabilisation against aggregation.

Stability of the AgNPs: The role of pH, DPPC and incubation time

TEM - morphological studies—The stability of AgNPs in the presence, or absence, of DPPC, at pH 3, 5 and 7 was monitored by measuring both the production of Ag^+ ions in solution and by assessing the morphological evolution of the AgNPs as a function of incubation time. The primary particle and aggregate sizes of AgNPs in their dry state were characterized using TEM (Figure 2a–n). The particle size distribution (PSD) became multimodal after t=168 hours, as AgNP dissolution and coarsening occurred (Figure 2o–r).

TEM imaging showed that AgNPs associated more rapidly with decreasing pH. AgNP aggregate sizes in pH 3 were significantly larger than in pH 5 and pH 7 (Figure 2). This implies that pH will affect the aggregation state of NPs in different cell culture media. Negligible changes in the aggregate sizes were measured at extracellular pH (~7.2) whereas the NPs tended to aggregate in lysosomal pH (~5.5). The PSD histograms (Figure 2(p–r)) illustrate a significant shift in the position of the peak maxima, *i.e.* from 16 nm at pH 7 to 32 nm at pH 5, and 44 nm at pH 3 after 7 days incubation, indicating that the particles aggregated, fused and *coarsened* significantly at lower pH.

TEM images also show that DPPC addition results in smaller clusters of NPs or isolated primary particles, which are redispersed within the DPPC. In DPPC, NP aggregation was strongly pH-dependent, with the size of aggregates increasing as pH decreases. In particular, Figure 2q and 2r showed a shift in the peak maxima of the PSD to smaller sizes in the presence of DPPC at pH 5 and 3, respectively. After 7 days incubation, the position of peak maxima shifted from 44 nm (without DPPC) to 24 nm (with DPPC) at pH 3, and from 32 nm (without DPPC) to 20 nm (with DPPC) at pH 5. This trend indicates that the phospholipid DPPC provides a more stable barrier between NPs, reducing NP interactions and inhibiting coarsening. At pH 7.0, there is no significant shift in size distribution between the samples with and without DPPC, indicating that DPPC stabilises the NPs dispersion, but does not affect the size distribution at neutral pH. This nano-bio interface is important in shaping the surface properties, charges, resistance to aggregation and hydrodynamic size of NPs.[39]

In order to study further the influence of pH and DPPC on particle aggregation state and morphology, TEM images of AgNPs incubated in solutions in the presence of DPPC were acquired at low (x 50 k) and high (x 100 k) magnification (Figure 3). Figure 3 shows the as-

prepared citrate- stabilised AgNPs. The NPs were wrapped by a thin layer of stabilising agent (citrate), approximately 1.4 ± 0.3 nm in thickness. By comparison, when NPs were incubated in solutions containing DPPC, there was a significant increase of capping layer thickness, which implies formation of DPPC layer(s) outside AgNPs/citrate, as shown in Figure 3c–d. The thickness difference of 4.2 ± 1.8 nm is close to a DPPC bilayer thickness of 5.5 nm, as determined by atomic force microscopy (AFM).[40] Leonenko[40] imaged a DPPC-supported bilayer using temperature-controlled AFM and demonstrated that thickness of DPPC bilayer varied as a function of temperature or analysis technique.

The detailed morphology of the DPPC layer(s) was further revealed using a uranyl acetate negative staining technique, which takes advantage of the high affinity of electron dense, uranyl ions, to the carboxyl groups of citrate and phosphate groups of DPPC, resulting in dark contrast.[41] The outside layer of NPs, which shows dark contrast, is likely to be the polar groups of the outer DPPC layer facing the aqueous environment (Figure 3e–f). The hydrophilic heads of the inner layer of DPPC likely interact with the citrate layer; however, it is difficult to absolutely define the boundary of the two layers (Figure 3f). A schematic model of the DPPC bilayer structure on AgNPs/citrate is illustrated in Figure 4. The thickness of the bilayer of DPPC hydrocarbon tails, not stained with uranium, show a bright contrast layer in between; this was determined to be 4.3 ± 0.6 nm (Figure 3f), close to the calculated hydrocarbon bilayer thickness of 4.16 nm. Further evidence for the existence of a lipid layer around AgNPs is provided by EDS analysis which shows the presence of phosphorus in samples immersed in DPPC.

ICP- OES - dissolution studies—Aliquots of Ag solutions were taken for ICP-OES analysis at various time points from 1 hour up to 14 days (336 hours). Dissolved silver appeared over the course of several hours up to two weeks. In the reaction, the dissolved silver was Ag^+ or Ag^+ complexed with anions (*i.e.* citrate), which can undergo dynamic exchange between surface bound and soluble forms.

Figure 5 shows that the Ag^+ release rate was strongly pH-dependent: increasing ion release rates were observed with decreasing pH. Negligible Ag^+ release (~ 0.4 %) was measured at pH 7, and ~ 2 % Ag^+ was released at pH 5, after 14 days (336 hours) incubation. At pH 3, considerable Ag^+ release was measured initially after 1 hour incubation; ~ 5 % of available Ag^+ ions had dissolved. The dissolution rate of the AgNPs subsequently decreased, and the amount of Ag^+ ions released gradually increased up to ~10 %, at 14 days.

For AgNPs incubated in DPPC, similar dissolution behaviour was observed compared to those incubated without DPPC (Figure 5). However, the DPPC appears to form a protective membrane, increasing AgNP chemical stability. At pH 3, < 1 % of AgNPs had dissolved after 1 hour incubation, compared to ~ 5 % released Ag^+ without DPPC. However, after 72 hours incubation at 37 °C (pH 3), the amount of dissolution was not significantly different from the samples without DPPC (Figure 2l and 2n). A similar trend was also observed at pH 5. Overall, DPPC imparted an initial retarding effect on the dissolution of AgNPs but the effect became less significant after two weeks of incubation at a given pH.

Comparisons of SAED patterns (Figure S5) in different media identified only the characteristic spacings of metallic silver.

Zeta potential (ξ) measurements—The dispersion surface charge of particles can be altered by changing the solution pH as shown in Figure 7. At the higher pH studied, the AgNPs suspension indicates a high ξ-magnitude of −32.5 mV, corresponding to a stable suspension. At lower pH, the magnitude decreases to −22.5 and −18.2 mV at pH 5 and 3, respectively; indicating weaker repulsive forces and a less stable suspension (Figure 6).

The ξ of AgNPs/citrate and DPPC-wrapped AgNPs were also investigated at different pH. Figure 6 shows that the ξ of AgNP/DPPC were smaller in magnitude compared to AgNPs without DPPC. ξ continued to decrease with pH, approaching isoelectric point (pI). However, despite the lower surface charge, the NPs are now stabilised by steric factors leading to more stable suspensions.

SAXS—Background-subtracted SAXS data are shown in Figure 7 along with fits to the data and extracted parameters. A good agreement between the data and fit was achieved for all the samples as indicated by the low χ^2 values. The extracted values for diameter D represent the average size of the scattering object: there is a dramatic increase in D for particles suspended in pH 3 and 5 solutions for a period of 9.5 h: from 18.6 nm to 39.1 nm and 55 nm for pH 5 and 3 respectively. Little change was observed for particles suspended in pH 7 solutions, in agreement with TEM analysis. Addition of DPPC to the solutions reduced the observed changes in D, although measurable differences were seen for both pH 5 and 3 (D=26.8 nm and 28.0 nm). This suggested that DPPC inhibits particle aggregation and coarsening, but may not fully prevent it. At pH 7, with DPPC there is no change in the SAXS analysis compared to as-prepared samples.

DISCUSSION

The overall goal of this study was to assess the effect of pH on the stability and aggregation state of AgNPs, and to determine how the presence of DPPC modifies these processes. In the secretory pathway, the pH decreases progressively from the endoplasmic reticulum (ER) lumen, (pH~7.1), early endosomes (pH~6.5) to late endosomes (pH<6.0) and, ultimately, lysosomes (pH<5.5).[42] A DPPC concentration of 100 mg.L^{-1} was chosen to mimic the concentration range of phospholipid in bronchoalveolar lavage fluid obtained from healthy adults.[13]

The aggregation state of NPs is an important consideration in controlling their reactivity in biological systems. A number of factors, including ionic strength, pH and surface chemistry, control both the propensity of NPs to aggregate and the aggregate size.[36,43] For any colloidal suspension an equilibrium is set up between the NP and solution, so even a simple Ag colloid will consist of three forms: AgNPs, free Ag^+ (including complexes), and surface-adsorbed silver Ag_{ads}. Here, TEM images show that NPs preferentially aggregate at pH 3 compared to pH 7 (Figure 2). This effect is related to the high [H^+] which causes charge screening (thus reducing electrostatic repulsion), and decreased intramolecular repulsion resulting in molecular shrinkage.[44] At any given pH, increasing the ionic strength

compresses the diffuse layer and decreases ξ of particles (Figure 6), thereby reducing intermolecular repulsion, leading to increased aggregation (Figure 8).[45–47,48]

The larger particle size observed at lower pH arises due to increased charge screening, which allows particles to agglomerate and then fuse by diffusion controlled coarsening, forming larger-sized particles. When particles are coated by citrate (pK_{a1}=3.13, pK_{a2}=4.76, pK_{a3}=6.40), they are electrostatically-stabilised by the negatively-charged anions. However, when the pH of the colloidal dispersion is decreased, protonation of citrate anions occurs, and the AgNPs are no longer electrostatically stabilised. Without their negative shell, the particles are not prevented from coming into close proximity, which allows growth of the particles. This effect can also be seen in Figures 2 (TEM) and 7 (SAXS), where the average particle diameter increases as the pH decreases.

The aggregation of extremely reactive NPs is driven by high surface energy and resultant thermodynamic instability of the NPs surface.[49] In suspension, Ag_{ads} will tend to diffuse between adjacent adsorption sites on a surface, forming bonds with nearest-neighbor atoms *via* Brownian diffusion.[50] In this reaction, the coarsening kinetics of the NPs are controlled by surface diffusion. As the system tends to lower its overall energy, smaller-sized particles will first agglomerate, then irreversibly fuse and coarsen to form large particles, decreasing the total energy of the system.[51]

In contrast, stable NPs dispersion requires a dominant interparticle repulsive force to prevent the adhesion of particles. The decreasing magnitude of ξ with pH (Figure 6) agrees well with the effects seen in TEM morphology studies. This supports the suggestion that larger aggregates found at lower pH may be due to the low surface charge and weak repulsive force when pH approaches the pI.[52] The ‘hard’ bonds of aggregates are difficult to break apart with agitation or ultrasonication due to a high energy barrier that hinders the separation of particles. When pH is far from the pI, the electrostatic repulsive force is high enough to counter the van der Waals force and prevent the aggregation of NPs, and *vice versa*.[53, 54]

In this study, the ICP results (Figure 5) show that NP dissolution rate increases with decreasing pH. Liu[55] found that dissolution of AgNPs is a cooperative effect of both dissolved oxygen and protons. In our study, dissolution was carried out in an ambient atmosphere, and therefore dissolved oxygen is a possible factor in the dissolution of AgNPs. Specifically, in a heterogeneous oxidation reaction, ion release is initiated by oxygen chemisorption accompanied by electron transfer. The Pourbaix diagram for Ag suggests that the equilibrium condition is not pH-dependent for acidic conditions, however it is clear from these data that the *kinetics* of dissolution are effected.[56] Protons in the fluid phase serve as a mediator and dissolution of NPs increases with higher $[H^+]$.[55] The global reaction stoichiometry is:

$$2Ag + 1/2\,O + 2H^+ \leftrightarrow 2Ag^+ + H_2O \quad (1)$$

For surfactant-coated NPs, the DPPC layer may act as a diffusion barrier to molecular oxygen, and thus decreases ion release kinetics and toxicity.[57] TEM analysis showed that the measured size distribution was biased towards small particles with the addition of DPPC,

indicating that DPPC improved the stability of the particles. This finding is in agreement with the result reported by Sager[14], who found that diluted alveolar lining fluid obtained through bronchoalveolar lavage improved the dispersion of ultrafine carbon black and TiO_2-NPs.

Since the TEM preparation method may cause drying-induced aggregation of the particles; measures have been taken to minimise such effects by placing a small drop of solution on to a Cu grid and drying under vacuum. Moreover, exactly the same protocol was used to dry all the samples, so if observed aggregation was related to such artefacts it would be expected for *all* the conditions studied. Therefore we are confident that the observed differences can only be attributed to the effects of the environmental test conditions. Although drying artefacts may create a systematic error, it cannot be disputed that significant differences between the aggregation states of AgNPs +/− DPPC, are observed. Furthermore; the *in-situ* SAXS measurement are consistent with our TEM data suggesting that such an approach (with appropriate care) is valid.

The ξ of AgNPs/citrate was reduced after lipid adsorption (Figure 6). This may be due to the positive charge of the hydrophilic headgroup of DPPC molecule $-N^{(+)}(CH_3)_3$ interacting with the negatively charged citrate coated AgNPs. Since DPPC is a zwitterion, the positive charge of ammonium group is favourable for electrostatic interaction with the AgNPs/citrate. Therefore, the presence of negative $-PO_3^-$ in the zwitterion may cause the relatively small decrease of surface charge which remains negative.[58]

The DPPC hydrophilic head group contains two oppositely charged groups[59]: a positively charged phosphate (P) group (1.8 nm) and a negatively charged choline (N) group (2 nm) as illustrated in Figure 4. The zwitterionic head group of DPPC with neutral charge over a wide pH range approximately from 4 to 10.[60] Despite its neutrality, DPPC carries a significant electric dipole moment and surface potential. Mashaghi[61] reported that the lipid headgroups of DPPC tightly bound to interfacial water molecules facilitates energy transfer across membranes[62]. This might explain the antifouling property of DPPC and the dispersion of NPs in DPPC suspension.[62] Moreover, when NPs interact with DPPC, the hydrophilic trimethyl ammonium and phosphate head group of the molecule is oriented outwards to the surrounding medium; this surface modification of a hydrophilic outer coating also allows the dispersion of the surfactant-coated AgNPs in aqueous media.[63]

Several reports have indicated that the cytotoxicity of nanosilver is decreased by the aggregation of AgNPs.[55, 64] Generally, NPs tend to aggregate into larger particles, decreasing the available surface area and decreasing reactivity.[65] Our present results show that the presence of DPPC maintains dispersion of NPs without significantly increasing the dissolution rates compared to those without DPPC (Figure 6); however DPPC did delay the release of silver ions. In principle, the ion release rate may also be inhibited by an increase in pH, oxygen depletion and high concentrations of free silver and free citrate.[66]

This study of the interaction of AgNPs with DPPC has provided an insight into the colloidal stability of these NPs in biologically relevant media under varying pH conditions. DPPC surfactant is the first line of defence against inhaled particles and helps to maintain

homeostasis of the airways. Over the range of pH values investigated, the results indicate that decreasing pH resulted in increased Ag^+ ion release and induced a much greater extent of aggregation and coarsening of the particles. TEM and *in situ* SAXS analysis showed that AgNPs did not aggregate or coarsen at extracellular pH; maintenance of their small size may allow them to enter cells (where NP dissolution and aggregation may subsequently occur). This may lead to a greater formation of ROS within cells, reduced cell viability, and increased DNA damage.

In conclusion, TEM images and *in situ* SAXS showed that AgNPs suspended in media containing DPPC were stabilised against coarsening and aggregation. Nevertheless, the presence of DPPC surfactant did not significantly affect the total amount of silver released over the pH range 3.0–7.0 after two weeks. These results enhance our understanding of the stability of NPs in the deep lung, and may be utilised for making predictions of how the aggregation state and stability of AgNPs changes in the LLF, thereby affecting the pulmonary system with regard to both respiratory physiology and host immunity. More generally, our results highlight the need to consider the interaction of engineered nanomaterials with biological molecules (in this case lipids) to understand the downstream effects in humans and the environment. In particular, detailed characterisation of whether, and how, engineered nanomaterials change in their physicochemical properties within a biological system or the environment will be essential to make informed predictions about the toxicity of engineered nanomaterials.

Supplementary Material

Refer to Web version on PubMed Central for supplementary material.

Acknowledgments

LBF is grateful for a PhD scholarship from the Ministry of Higher Education of Malaysia. This work was funded in part by grants from the NIEHS (U19ES019536) and the US EPA/NERC (EPA STAR RD83469301 and NERC). AP acknowledges an ERC starting grant (# 257182) for additional support with electron microscopy characterisation. This work was carried out with the support of the Diamond Light Source (Experiment SM7775).

References

1. Kim JS, Kuk E, Yu KN, Kim JH, Park SJ, Lee HJ, Kim SH, Park YK, Park YH, Hwang CY, Kim YK, Lee YS, Jeong DH, Cho M-H. Antimicrobial effects of silver nanoparticles. Nanomedicine-Nanotechnology Biology and Medicine. 2007; 3(1):95–101.
2. Dirix Y, Bastiaansen C, Caseri W, Smith P. Oriented pearl-necklace arrays of metallic nanoparticles in polymers: A new route toward polarization-dependent color filters. Advanced Materials. 1999; 11(3):223.
3. Wiley B, Sun Y, Xia Y. Synthesis of silver wanostructures with controlled shapes and properties. Accounts of Chemical Research. 2007; 40(10):1067–1076. [PubMed: 17616165]
4. Ma PC, Tang BZ, Kim JK. Effect of CNT decoration with silver nanoparticles on electrical conductivity of CNT-polymer composites. Carbon. 2008; 46(11):1497–1505.
5. Benn TM, Westerhoff P. Nanoparticle silver released into water from commercially available sock fabrics. Environmental Science & Technology. 2008; 42(11):4133–4139. [PubMed: 18589977]
6. Hussain SM, Schlager JJ. Safety Evaluation of Silver Nanoparticles: Inhalation Model for Chronic Exposure. Toxicological Sciences. 2009; 108(2):223–224. [PubMed: 19237550]

7. Park J, Lim DH, Lim HJ, Kwon T, Choi JS, Jeong S, Choi IH, Cheon J. Size dependent macrophage responses and toxicological effects of Ag nanoparticles. Chemical Communications. 2011; 47(15): 4382–4384. [PubMed: 21390403]
8. Li JJ, Muralikrishnan S, Ng CT, Yung LYL, Bay BH. Nanoparticle-induced pulmonary toxicity. Experimental Biology and Medicine. 2010; 235(9):1025–1033. [PubMed: 20719818]
9. Buzea C, Pacheco II, Robbie K. Nanomaterials and nanoparticles: Sources and toxicity. Biointerphases. 2007; 2(4):MR17–MR71. [PubMed: 20419892]
10. Tetley TD. Health effects of nanomaterials. Biochemical Society. 2007; 35(3):527–531.
11. Rooney SA, Young SL, Mendelson CR. Molecular and cellular processing of lung surfactant. Faseb Journal. 1994; 8(12):957–967. [PubMed: 8088461]
12. Creuwels L, vanGolde LMG, Haagsman HP. The pulmonary surfactant system: Biochemical and clinical aspects. Lung. 1997; 175(1):1–39. [PubMed: 8959671]
13. Griese M. Pulmonary surfactant in health and human lung diseases: state of the art. European Respiratory Journal. 1999; 13(6):1455–1476. [PubMed: 10445627]
14. Sager TM, Castranova V. Surface area of particle administered versus mass in determining the pulmonary toxicity of ultrafine and fine carbon black: comparison to ultrafine titanium dioxide. Particle and Fibre Toxicology. 2009:6. [PubMed: 19284582]
15. Veldhuizen R, Nag K, Orgeig S, Possmayer F. The role of lipids in pulmonary surfactant. Biochimica Et Biophysica Acta-Molecular Basis of Disease. 1998; 1408(2–3):90–108.
16. Goerke J, Gonzales J. Temperature-dependence of dipalmitoylphosphatidylcholine monolayer stability. Journal of Applied Physiology. 1981; 51(5):1108–1114. [PubMed: 6895370]
17. Zuo YY, Possmayer F. How does pulmonary surfactant reduce surface tension to very low values? Journal of Applied Physiology. 2007; 102(5):1733–1734. [PubMed: 17303712]
18. Notter, RH. Lung Surfactants:Basic Science and Clinical Applications. Marcel Dekker; New York: 2000.
19. Richter R, Mukhopadhyay A, Brisson A. Pathways of lipid vesicle deposition on solid surfaces: A combined QCM-D and AFM study. Biophysical Journal. 2003; 85(5):3035–3047. [PubMed: 14581204]
20. McConnell HM, Watts TH, Weis RM, Brian AA. Supported planar membranes in studies of cell-cell recognition in the immune-system. Biochimica Et Biophysica Acta. 1986; 864(1):95–106. [PubMed: 2941079]
21. Roiter Y, Ornatska M, Rammohan AR, Balakrishnan J, Heine DR, Minko S. Interaction of nanoparticles with lipid membrane. Nano Letters. 2008; 8(3):941–944. [PubMed: 18254602]
22. Wang B, Zhang L, Bae SC, Granick S. Nanoparticle-induced surface reconstruction of phospholipid membranes. Proceedings of the National Academy of Sciences of the United States of America. 2008; 105(47):18171–18175. [PubMed: 19011086]
23. Guzman E, Liggieri L, Santini E, Ferrari M, Ravera F. Effect of Hydrophilic and Hydrophobic Nanoparticles on the Surface Pressure Response of DPPC Monolayers. Journal of Physical Chemistry C. 2011; 115(44):21715–21722.
24. Porter D, Sriram K, Wolfarth M, Jefferson A, Schwegler-Berry D, Andrew M, Castranova V. A biocompatible medium for nanoparticle dispersion. Nanotoxicology. 2008; 2(3):144–154.
25. Sager TM, Porter DW, Robinson VA, Lindsley WG, Schwegler-Berry DE, Castranova V. Improved method to disperse nanoparticles for in vitro and in vivo investigation of toxicity. Nanotoxicology. 2007; 1(2):118–129.
26. MacCuspie RI, Allen AJ, Hackley VA. Dispersion stabilization of silver nanoparticles in synthetic lung fluid studied under in situ conditions. Nanotoxicology. 2011; 5(2):140–156. [PubMed: 21609136]
27. Bakshi MS, Zhao L, Smith R, Possmayer F, Petersen NO. Metal nanoparticle pollutants interfere with pulmonary surfactant function in vitro. Biophysical Journal. 2008; 94(3):855–868. [PubMed: 17890383]
28. Yang ST, Liu Y, Wang YW, Cao A. Biosafety and Bioapplication of Nanomaterials by Designing Protein-Nanoparticle Interaction. Small. 2013

29. Wells MA, Abid A, Kennedy IM, Barakat AI. Serum proteins prevent aggregation of Fe2O3 and ZnO nanoparticles. Nanotoxicology. 2012; 6(8):837–846. [PubMed: 22149273]
30. Harishchandra RK, Saleem M, Galla HJ. Nanoparticle interaction with model lung surfactant monolayers. J R Soc Interface. 2010; 7:S15–S26. [PubMed: 19846443]
31. Stebounova LV, Guio E, Grassian VH. Silver nanoparticles in simulated biological media: a study of aggregation, sedimentation, and dissolution. Journal of Nanoparticle Research. 2011; 13(1): 233–244.
32. Yin LY, Cheng YW, Espinasse B, Colmam BP, Auffan M, Wierner M, Rose J, Liu J, Bernhardt ES. More than the ions: The effect of Silver Nanoparticles on Lodium multiflorum. Environ Sci Technol. 2011; 45:2360–2367. [PubMed: 21341685]
33. El Badawy AM, Silva RG, Morris B, Scheckel KG, Suidan MT, Tolaymat TM. Surface Charge-Dependent Toxicity of Silver Nanoparticles. Environmental Science & Technology. 2011; 45(1): 283–287. [PubMed: 21133412]
34. Levard C, Reinsch BC, Michel FM, Oumahi C, Lowry GV, Brown GE. Sulfidation Processes of PVP-Coated Silver Nanoparticles in Aqueous Solution: Impact on Dissolution Rate. Environmental Science & Technology. 2011; 45(12):5260–5266. [PubMed: 21598969]
35. Park HJ, Kim JY, Kim J, Lee JH, Hahn JS, Gu MB, Yoon J. Silver-ion-mediated reactive oxygen species generation affecting bactericidal activity. Water Research. 2009; 43(4):1027–1032. [PubMed: 19073336]
36. Elzey S, Grassian VH. Agglomeration, isolation and dissolution of commercially manufactured silver nanoparticles in aqueous environments. Journal of Nanoparticle Research. 2010; 12(5): 1945–1958.
37. Muller KH, Kulkarni J, Motskin M, Goode A, Winship P, Skepper JN, Ryan MP, Porter AE. pH-Dependent Toxicity of High Aspect Ratio ZnO Nanowires in Macrophages Due to Intracellular Dissolution. Acs Nano. 2010; 4(11):6767–6779. [PubMed: 20949917]
38. AshaRani PV, Mun GLK, Hande MP, Valiyaveettil S. Cytotoxicity and Genotoxicity of Silver Nanoparticles in Human Cells. Acs Nano. 2009; 3(2):279–290. [PubMed: 19236062]
39. Cedervall T, Lynch I, Lindman S, Berggard T, Thulin E, Nilsson H, Dawson KA, Linse S. Understanding the nanoparticle-protein corona using methods to quantify exchange rates and affinities of proteins for nanoparticles. Proceedings of the National Academy of Sciences of the United States of America. 2007; 104(7):2050–2055. [PubMed: 17267609]
40. Leonenko ZV, Finot E, Ma H, Dahms TE, Cramb DT. Investigation of temperature-induced phase transitions in DOPC and DPPC phospholipid bilayers using temperature-controlled scanning force microscopy. Biophys J. 2004; 86(6):3783–93. [PubMed: 15189874]
41. Hayat, MA. Principles and Techniques of Electron Microscopy Biological Applications. 4. Cambridge University Press; 2000. p. 545
42. Demaurex N. pH homeostasis of cellular organelles. News in Physiological Sciences. 2002; 17:1–5. [PubMed: 11821527]
43. Chen KL, Elimelech M. Influence of humic acid on the aggregation kinetics of fullerene (C60) nanoparticles in monovalent and divalent electrolyte solutions. Journal of Colloid and Interface Science. 2007; 309(1):126–134. [PubMed: 17331529]
44. Avena MJ, Vermeer AWP, Koopal LK. Volume and structure of humic acids studied by viscometry pH and electrolyte concentration effects. Colloids and Surfaces a-Physicochemical and Engineering Aspects. 1999; 151(1–2):213–224.
45. French RA, Jacobson AR, Kim B, Isley SL, Penn RL, Baveye PC. Influence of Ionic Strength, pH, and Cation Valence on Aggregation Kinetics of Titanium Dioxide Nanoparticles. Environmental Science & Technology. 2009; 43(5):1354–1359. [PubMed: 19350903]
46. Jin X, Li M, Wang J, Marambio-Jones C, Peng F, Huang X, Damoiseaux R, Hoek EMV. High-Throughput Screening of Silver Nanoparticle Stability and Bacterial Inactivation in Aquatic Media: Influence of Specific Ions. Environmental Science & Technology. 2010; 44(19):7321–7328. [PubMed: 20873875]
47. Lead JR, Wilkinson KJ, Starchev K, Canonica S, Buffle J. Determination of diffusion coefficients of humic substances by fluorescence correlation spectroscopy: Role of solution conditions. Environmental Science & Technology. 2000; 34(7):1365–1369.

48. Delay M, Dolt T, Woellhaf A, Sembritzki R, Frimmel FH. Interactions and stability of silver nanoparticles in the aqueous phase: Influence of natural organic matter (NOM) and ionic strength. Journal of Chromatography A. 2011; 1218(27)
49. Olenin AY, Krutyakov YA, Kudrinskii AA, Lisichkin GV. Formation of surface layers on silver nanoparticles in aqueous and water-organic media. Colloid Journal. 2008; 70(1):71–76.
50. Ball RC, Weitz DA, Witten TA, Leyvraz F. Universal kinetics in reaction-limited aggregation. Physical Review Letters. 1987; 58(3):274–277. [PubMed: 10034887]
51. Chen KL, Elimelech M. Aggregation and deposition kinetics of fullerene (C-60) nanoparticles. Langmuir. 2006; 22(26):10994–11001. [PubMed: 17154576]
52. Petosa AR, Jaisi DP, Quevedo IR, Elimelech M, Tufenkji N. Aggregation and Deposition of Engineered Nanomaterials in Aquatic Environments: Role of Physicochemical Interactions. Environmental Science & Technology. 2010; 44(17):6532–6549. [PubMed: 20687602]
53. Sperling RA, Parak WJ. Surface modification, functionalization and bioconjugation of colloidal inorganic nanoparticles. Phil Trans R Soc A. 2009; 368:1333–1383. [PubMed: 20156828]
54. Phenrat T, Saleh N, Sirk K, Kim HJ, Tilton RD, Lowry GV. Stabilization of aqueous nanoscale zerovalent iron dispersions by anionic polyelectrolytes: adsorbed anionic polyelectrolyte layer properties and their effect on aggregation and sedimentation. J Nanopart Res. 2008; 10:795–814.
55. Liu JY, Hurt RH. Ion Release Kinetics and Particle Persistence in Aqueous Nano-Silver Colloids. Environmental Science & Technology. 2010; 44(6):2169–2175. [PubMed: 20175529]
56. Takeno N. Atlas of Eh-pH Diagrams. 2005 May.
57. Zhang W, Yao Y, Li KG, Huang Y, Chen YS. Influence of dissolved oxygen on aggregation kinetics of citrate-coated silver nanoparticles. Environmental Pollution. 2011; 159(12):3757–3762. [PubMed: 21835520]
58. Chibowski E, Szczes A, Holysz L. Changes of zeta potential and particles size of silica caused by DPPC adsorption and enzyme phospholipase A(2) presence. Adsorption-Journal of the International Adsorption Society. 2010; 16(4–5):305–312.
59. Langner M, Kubica K. The electrostatics of lipid surfaces. Chemistry and Physics of Lipids. 1999; 101:3–35. [PubMed: 10810922]
60. Jones MN. The surface-properties of phospholipid liposome systems and their characterization. Advances in Colloid and Interface Science. 1995; 54:93–128. [PubMed: 7832999]
61. Mashaghi A, Partovi-Azar P, Jadidi T, Nafari N, Maass P, Tabar MRR, Bonn M, Bakker HJ. Hydration strongly affects the molecular and electronic structure of membrane phospholipids. Journal of Chemical Physics. 2012; 136(11)
62. Mashaghi A, Partovi-Azar P, Jadidi T, Nafari N, Esfarjani K, Maass P, Tabar MRR, Bakker HJ, Bonn M. Interfacial Water Facilitates Energy Transfer by Inducing Extended Vibrations in Membrane Lipids. Journal of Physical Chemistry B. 2012; 116(22):6455–6460.
63. Porter D, Sriram K, Wolfarth M, Jefferson A, DSB, Andrew ME, Castranova V. A compatible medium for nanoparticle dispersion. Nanotoxicology. 2008; 2:144–154.
64. Bae E, Park HJ, Lee J, Kim Y, Yoon J, Park K, Choi K, Yi J. Bacteria cytotoxicity of the silver nanoparticle related to physicochemical metrics and agglomeration properties. Environmental Toxicology and Chemistry. 2010; 29(10):2154–2160. [PubMed: 20872676]
65. Gebel E. The Mysterious Fates of Nanoparticles: ES&T's Top Feature Article 2012. Environ Sci Technol. 2013
66. Damm C, Munstedt H. Kinetic aspects of the silver ion release from antimicrobial polyamide/silver nanocomposites. Applied Physics a-Materials Science & Processing. 2008; 91(3):479–486.
67. Derjaguin BV, Landau L. Theory of the stability of strongly charged lyophobic sols and of the adhesion of strongly charged particles in solution of electrolytes. Acta Physicochimica (USSR). 1941; 14:633.
68. Verwey, EJW.; Overbeek, JTG. Theory of the stability of lyophobic colloids. Elsevier; Amsterdam: 1948.

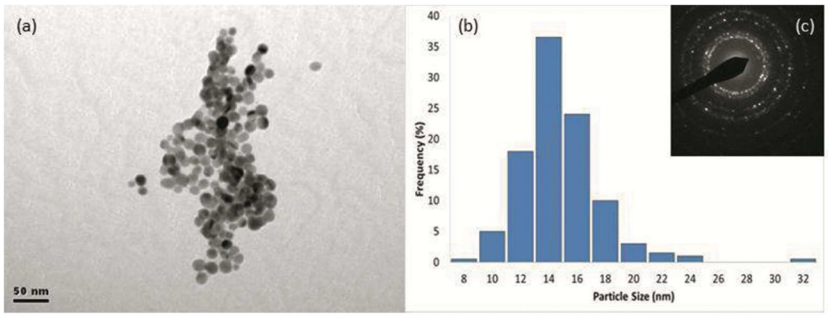

Figure 1.

(a) Bright-field TEM image of as-prepared AgNPs. (b) Corresponding size distribution (n=200), and (c) SAED pattern (camera length=30 cm) taken from AgNPs prepared by $NaBH_4$ reduction. (Indexed patterns are included in the Supporting information).

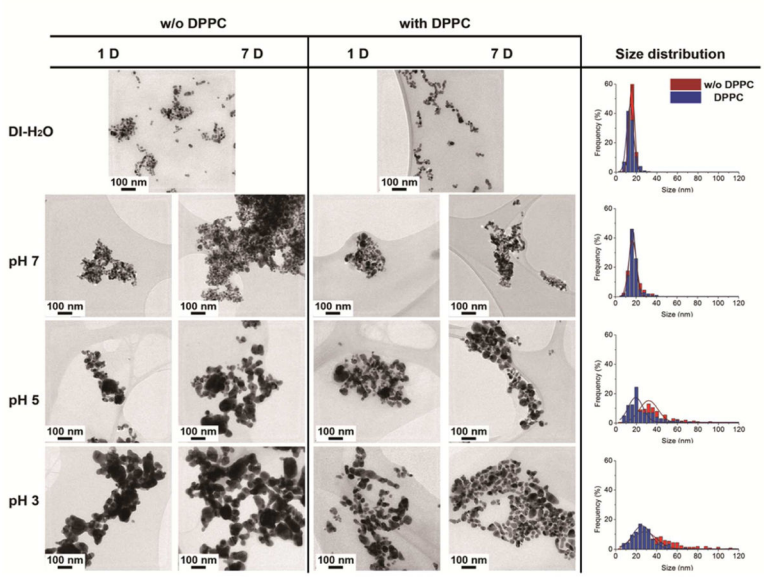

Figure 2.

TEM images of AgNPs incubating in water suspension (a–b) and aqueous suspension at pH 7 (c–f), pH 5 (g–j), and pH 3 (k–n) with magnification of 20k and their particle size distribution (N=200) histograms (o–r) were measured from TEM images in the presence, and absence, of DPPC after 7 days incubation.

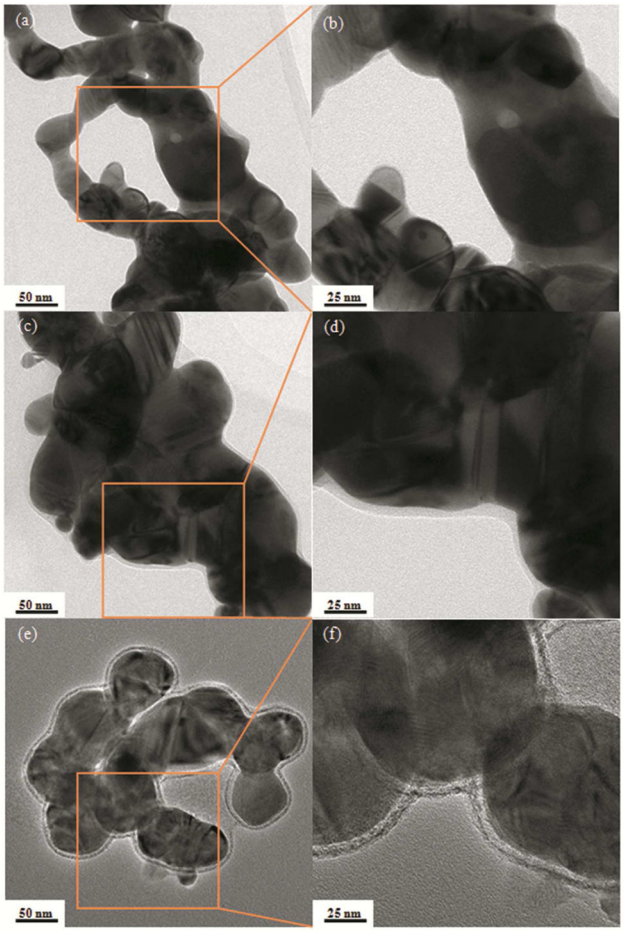

Figure 3.
TEM images for AgNPs incubated in pH 3 solution) in the absence (a and b), and in the presence (c and d) of DPPC, for 1 day. Samples negatively stained with uranyl acetate (e and f) to enhance contrast of lipid coating.

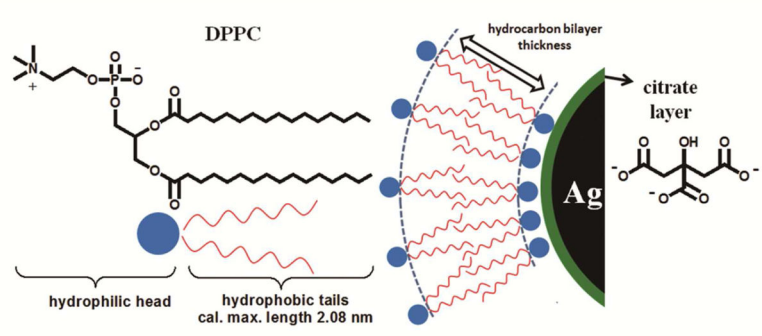

Figure 4.

A schematic illustration of a model of DPPC bilayer structure coated outside citrate stabilized AgNPs. The DPPC surfactant molecule consists of a trimethyl ammonium bounded to an acidic phosphate, providing a hydrophilic zwitterionic head group and two hydrophobic fatty acid tails comprised by 16 hydrocarbons. There is likely formation of a lipid bilayer structure on the surface of citrate coated AgNPs, with hydrophobic tails associating with each other, whereas hydrophilic groups of two layers oriented toward to aqueous environment and citrate layer respectively. The hydrocarbon bilayer thickness was determined by TEM analysis through negative staining.

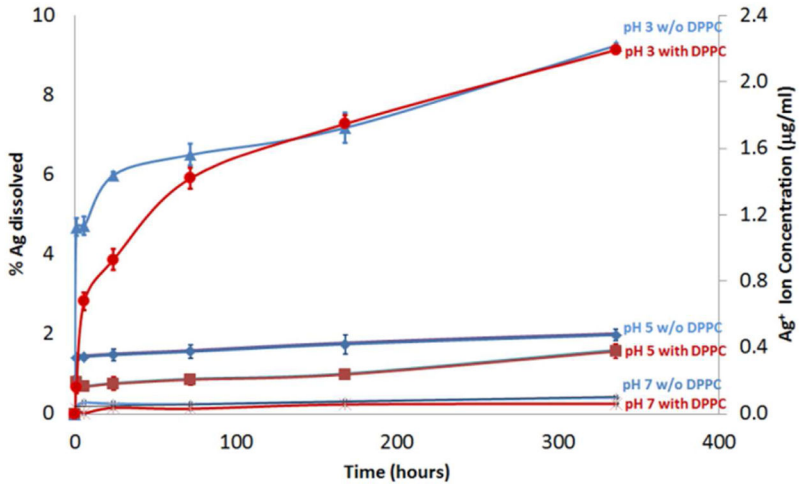

Figure 5.

Ag^{+} ion release study of AgNPs incubated in perchlorate acid/perchlorate buffer solutions (pH 3, 5, and 7) in the presence, and absence of DPPC.

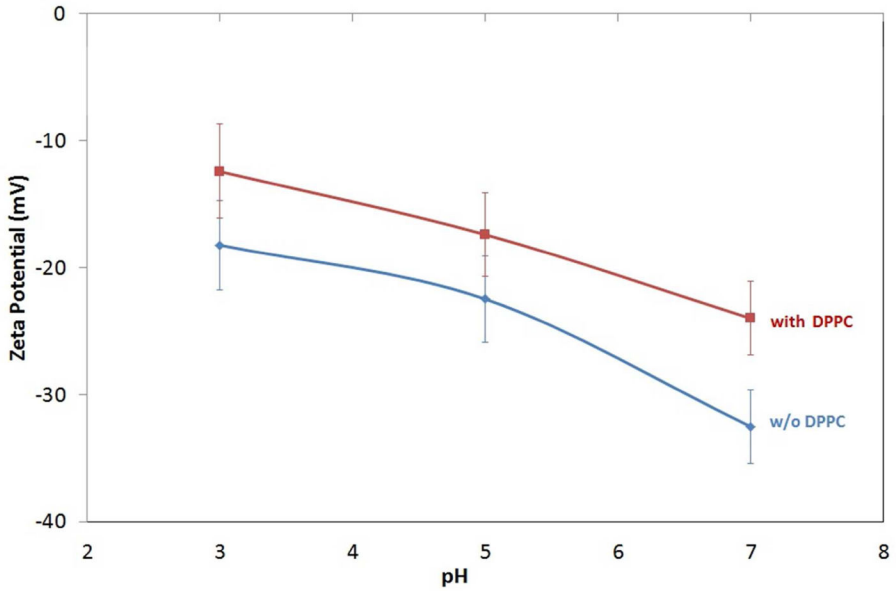

Figure 6.

Surface charge of AgNPs incubated in the suspension (with and without DPPC) as a function of pH

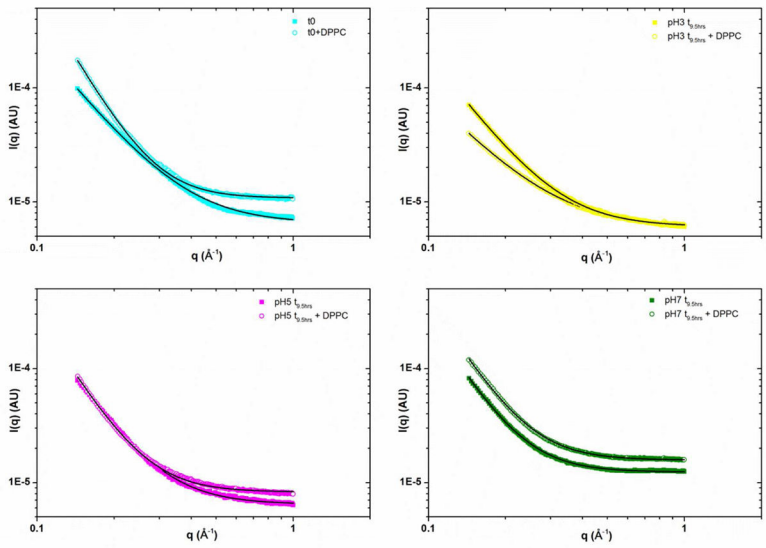

	As made, t=0		pH3, t=9.5 hrs		pH5, t=9.5 hrs		pH7, t=9.5 hrs	
	-DPPC	+DPPC	-DPPC	+DPPC	-DPPC	+DPPC	-DPPC	+DPPC
R_g (nm)	7.1	7.0	21.3	10.9	15.1	10.4	7.7	7.0
D (nm)	18.6	18.0	55.0	28.0	39.1	26.8	19.8	18.8
χ^2 (x 10^{-13})	1.2	2.3	0.5	0.5	1.0	1.3	0.6	1.6

Figure 7.

In-situ small angle X-ray scattering of NPs suspended in various pH solutions with and without DPPC; data (symbols) and fits (lines) along with extracted data.

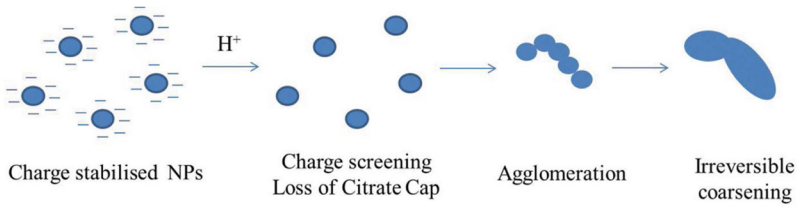

Figure 8.

Schematic representation of the aggregation process for citrate-stabilised AgNPs. AgNPs are stabilised by an electrostatic repulsive force between particles. Aggregation occurs with the increasing of pH due to the protonation of citrate anions, which can be elucidated by Derjaguin-Landau-Verwey-Overbeek (DLVO) theory.[67, 68]